Bathtub Vortex Generated by Tangential Jet Injection in a Vertical Tube and its Prevention by Flow Control Devices

Jason Ward, Naphatsorn Vongsoasup, Patrapol Tangchitnamthamrong, Paveen Padungruengkit, Asi Bunyajitradulya*

Department of Mechanical Engineering, Faculty of Engineering, Chulalongkorn University
Bangkok 10330, Thailand
* Corresponding Author: E-mail: asi.b@chula.ac.th , Tel: 02 218 6645, Fax: 02 218 6645

Abstract

The condition under which a bathtub vortex is formed and the characteristics of the formed bathtub vortex generated by tangential jet injection at the bottom of a vertical tube with draining orifice are investigated. This is an extension of our earlier work, which i) identified five flow regimes, namely, Regime 1: vertically steady, full-time fully-stretched vortex ($h/H=1$); Regime 2: vertically oscillating, part-time fully-stretched vortex ($0<h/H<=1$); Regime 3: vertically steady, full-time partially-stretched vortex with bubble detachment ($0<h/H<1$); Regime 4: vertically steady, full-time partially-stretched vortex without bubble detachment ($0<h/H<1$); and Regime 5: no bathtub vortex ($h/H\approx 0$), where *h/H* is the vortex stretching ratio, the ratio of the depth of the vortex air core to the water level, and ii) found the collapse of the relations between *h/H* and the jet Reynolds number Re_j at various diametric swirl ratios Sr_d, independent of both Re_j and Sr_d separately, when *h/H* is correlated instead with the new variable $\alpha = \mathrm{Re}_j/Sr_d$. In this work, i) we extend the range of α from upto 15,000 to upto 27,000, and ii) we investigate the effectiveness of flow control devices that can potentially be used to prevent the formation of the bathtub vortex. An experiment is conducted via flow visualization. Our findings are as follows. i) By identifying each flow regime with the vortex stretching ratio *h/H*, the condition for the formation of bathtub vortex in each flow regime is found to correlate reasonably well with the parameter α. ii) The collapses of the vortex stretching ratio *h/H* and the normalized water level *H/d* against α, independent of both Re_j and Sr_d, are confirmed but with some discrepancy from the earlier work. As a result, additional parameters that potentially affect *h/H*-α relation are discussed. iii) An additional flow pattern, namely, Flow Pattern 6: the vertically oscillating, part-time 'reverse vortex,' is identified. iv) The flow control device in the shape of a small strip installed at either the topmost position near the free surface or the bottommost position near the orifice is both found to be effective in preventing bathtub vortex formation completely. In addition, the fact that a relatively small strip is effective at both these extreme positions suggests that the condition for its formation is localized in the vertical cylindrical region centered on the container axis and that an effective flow control scheme for its prevention can focus on a localized disturbance in this localized region. Finally, many bathtub vortex related phenomena such as the oscillation of water level in flow Regimes 2 and flow Pattern 6, and the reduction in water level when flow control device is installed and the vortex air core gotten rid of, are identified and explained in terms of the blockage area ratio when the vortex air core is present at the orifice.

Keywords: bathtub vortex, tangential jet, Reynolds number, swirl ratio, flow control

1. Introduction

Bathtub vortex is a common flow phenomena that is observed, for example, when water is drained in a tank. Under appropriate condition, the free surface is deformed, resulting in a bell-mouthed funnel air core stretching from the above free surface vertically down towards the bottom orifice. When this deformation of the free surface occurs, the so-called 'bathtub vortex' is formed.

In applications, bathtub vortex can be found in, e.g., a tank on the suction side of a pump. In this case, it is generally undesirable to have a bathtub vortex since it interferes with the operation of the pump and can cause damage to the pump. Care in the system design and installation of the pump must be taken to ensure that the condition for its formation is avoided; or, if it is unavoidable, appropriate flow control

device can be easily deployed to prevent its formation.

In this regard, two immediate questions arise: 1) under what condition a bathtub vortex can form; and, if it does form, how many forms it can manifest, and 2) if this condition is unavoidable, what flow control device can be used to prevent its formation.

While many factors influence the formation of a bathtub vortex and the formed bathtub vortex can be stationary or intermittent, the two prominent parameters for the presence of the bathtub vortex are the tangential and axial velocities. In this regard, while in nature the formation of bathtub vortex is often intermittent and the source of tangential velocity may not be apparent (e.g., velocity disturbance, coriolis force), the generation of bathtub vortex in laboratories can be either intermittent or stationary and the source of tangential velocity is often imposed by, e.g., rotating container, shear flow configuration, tangential jet injection. The axial velocity is often induced by gravity, usually by the presence of a drain hole at the bottom of a container below the free surface.

Past works have addressed various aspects regarding bathtub vortex (structures and characteristics, field properties, etc.), in various configurations (besides rotating container, etc., mentioned above, infinite domain), and with various approaches (theoretical, experimental, modeling and simulation).

Andersen *et al*. [2; see also 3] studied a stationary bathtub vortex generated by a rotating cylindrical container with bottom outflow orifice and circumferential, inflow inlet located on the side wall near the bottom of the container. Water level was kept constant, and flow visualization was used. At approximately constant rate of outflow, they found that as the rotational speed increased, the free surface deformation increased by further extending downward, resulting in a central needlelike shaped air core extending downward. As the rotational speed increased further, the tip of the free surface deformation was no longer stable: air bubbles detached from the tip and were dragged down by the surrounding flow. When the rotational speed increased even further, the bubble shedding frequency increased until the air core extended all the way down through the drain hole. (In this regard, excluding the case of no bathtub vortex, essentially three flow regimes could be identified: Regimes 4, 3, and 1, respectively. See further discussions in Sec 7: Discussions.) They also provided a theoretical analysis for a stationary bathtub vortex in a rotating container. By modifying the model of Lundgren [4] by including the effects of Ekman upflow and surface tension, they found that the new model more accurately described the free surface and azimuthal velocity profiles.

Bergmann *et al*. [5] used the same flow configuration to study the pinch-off of air bubbles in a stationary bathtub vortex, noting that the bubble shedding phenomena in bathtub vortex could potentially be used as a bubble generator. They found that in the bubbling state, the bubble shedding frequency increased and the bubble size decreased with increasing rotational speed.

Ezure *et al*. [6] studied intermittent bathtub vortex and investigated the distributions of the entrained bubble diameters and shapes for (the prevention of) gas entrainment in nuclear reactors. Intermittent bathtub vortex was generated using a shear flow configuration in an open channel with two spanwisely located cavities. The two cavities were divided by two splitter plates on the upstream and downstream ends, leaving the center portions of the two cavities exposed and connected. At this center region between the two cavities located a suction nozzle at the bottom floor. The tangential velocity was then generated by allowing water to flow along in only one cavity; the other cavity was closed at both upstream and downstream ends and the water in it stagnant. The axial velocity was generated by the bottom suction nozzle. Water level was also kept constant in this experiment. Excluding the case of no bathtub vortex, they reported three intermittent flow patterns, in their terminology: dimple, Type I, and Type II. For the dimple, gas core was formed, but no gas entrainment (no bubble detachment); Type I, gas core was formed, with bubble detachment; Type II, gas core was formed and extended to the suction nozzle. In addition, the relative frequency of the occurrences of these intermittent flow regimes depended on the relative magnitude of the tangential and axial velocities. Specifically, they found that the relative increase in axial velocity resulted in the shift of the frequency of occurrence from Type-I dominated to Type-II dominated. On the other hand, the relative increase in the tangential velocity resulted in the increase in the frequency of occurrence of the dimple.

Rumpirujipong and Bunyajitradulya [1] observed that the flow configurations such as rotating container [2,3,5], shear flow configure-tion [6], and vertical planar tangential jet [7], used in past works resulted in the ‘forcing’ tangential velocity being uniformly distributed

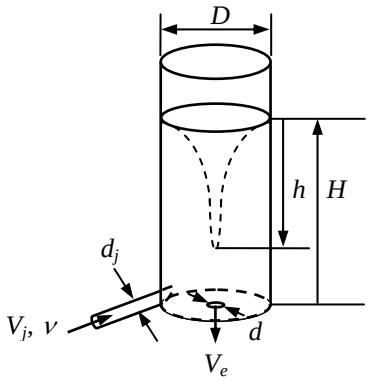

Fig. 1. Configuration of the test tube and the governing dimensional parameters.

over the depth of fluid, from the top free surface down to the bottom orifice. Under the premise that, to first-order approximation, if the axial and tangential velocities were ones of the most dominant parameters that governed the formation of bathtub vortex, the configuration for the generation and the condition of the tangential velocity should play secondary role so long as the suitable condition for the two velocities was established. With this premise, they chose to study a stationary bathtub vortex generated by a circular tangential jet injection at the bottom of a vertical tube with bottom orifice. The flow configuration is shown in Fig. 1. As a result, their work differed from past works in two aspects. Firstly, while they still used a bottom orifice to generate the axial velocity, their use of a circular jet injected tangentially at the bottom resulted in a 'point' source of forcing located only at the bottom, as opposed to the uniform forcing along the water depth like earlier works. In addition, the no-slip condition along the vertical tube wall further diminished the forcing tangential velocity, as opposed to further reinforced it along the water depth like earlier works. Secondly, unlike past works that kept water level as a control, independent parameter and constant, they left water level as an uncontrolled variable and measured it as a dependent variable.

With the above flow configuration, they identified five flow regimes: from Regime 1: vertically steady, full-time fully-stretched vortex ($h/H = 1$) to Regime 4: vertically steady, full-time partially-stretched vortex without bubble detachment ($0 < h/H < 1$); and Regime 5: no bathtub vortex ($h/H \approx 0$). (See further details of these five flow regimes in Sec 4.1.) h/H is the '*vortex stretching ratio*,' the ratio of the depth of the vortex air core (h) to the water level (H). In addition, they found the collapse of the relations between h/H and the jet Reynolds number Re_j at various diametric swirl ratios Sr_d when h/H is correlated instead with the new variable $\alpha = \mathrm{Re}_j/Sr_d$, independent of both Re_j and Sr_d separately. These variables will be defined more clearly in Sec 2. In their work, the range of Re_j is upto 40,000 and Sr_d's are 0.8, 2.0, and 4.0, resulting in the range of α upto 15,000.

With the two posted questions above and following [1], our present work has two main objectives. Firstly, the condition for the formation of a bathtub vortex and the characteristics of the formed bathtub vortex generated by tangential jet injection at the bottom of a vertical tube with draining orifice are investigated, in an extended range of α, from upto 15,000 in [1] to upto 27,000, about twice as large. In addition, by extending the range of α and using a new setup, the validity of the collapse of h/H against α in a wider range of α and in a different setup is also investigated. Secondly, the effectiveness of a few flow control devices for the prevention of the formation of such bathtub vortex is investigated. For continuity, some of the materials in [1] are reviewed in Secs. 2, 4.1, and 4.2.

2. Governing Dimensionless Parameters

It is postulated that, to first-order approximation, the dimensional variables that govern the depth of the vortex air core measured from the free surface (h) and the water level in the tube measured from the tube floor (H) are the diameter of the tube (D), the diameter of the orifice (d), the diameter of the jet (d_j), the velocity of the jet (V_j), the kinematic viscosity of the fluid (ν), and the density of the fluid (ρ); see Fig. 1. The axial exit velocity at the orifice (V_e), like h and H, is the dependent variable in this case. The problem can then be written in functional form as

$$h, H = f(D, d, d_j, V_j, \nu, \rho). \qquad (1')$$

When analyze the dimensions of Eq. (1′), we find

$$\left.\begin{matrix} h/d_j \\ H/d_j \end{matrix}\right\} = f(V_j d_j/\nu; d/d_j; D/d_j). \qquad (2')$$

From Eqs. (1′) and (2′), it is observed that since ρ is the only variable with the dimension of mass (M) and the remaining variables have the dimensions of length (L) and time (t) only, it cannot form a dimensionless parameter with the remaining variables. Thus, this suggests that ρ has secondary or no effect in this flow. We then revise Eq. (1′) as

$$h, H = f(D, d, d_j, V_j, \nu), \qquad (1)$$

and, for convenience in physical interpretation, rearrange the dimensionless parameters in Eq. (2′) as

$$\left.\begin{matrix} h/H \\ H/d \end{matrix}\right\} = f(V_j d_j/\nu; d/d_j; D/d_j), \qquad (2)$$

where, in place of d_j, H and d are chosen instead to normalize h and H, respectively.

Here, we use the 3-slot semicolon convention in the functional form, $y = f(...,...;...,...;...,...)$, to differentiate different roles of variables in the experiment. Namely, the variables on the left-hand side, e.g., h/H and H/d, are considered dependent variables. The variables in the first slot before the first semicolon in the parentheses (there can be more than one variable), e.g., $V_j d_j/\nu$, are considered the *independent variables* that will be varied in the experiment. The variables in the second slot in between the two semicolons, e.g., d/d_j, are considered *variable parameters* that will also be varied in the experiment as the index of the family, or case, of experiments. Finally, the variables in the last slot after the second semicolon are considered *constant parameters*, which will be fixed constant throughout the experiment.

Applying the conservation of mass in an average sense, we have $V_j/V_e = (d/d_j)^2$. Anticipating the importance of the tangential to axial velocity ratio or the *swirl ratio*, $Sr = V_j/V_e$, we define the *diametric swirl ratio* as $Sr_d = (d/d_j)^2$, which gives $Sr = Sr_d$, and use Sr_d in place of d/d_j in Eq. (2). Finally, we rewrite Eq. (2) as

$$\left.\begin{matrix} h/H \\ H/d \end{matrix}\right\} = f(\mathrm{Re}_j; Sr_d; D/d_j) \qquad (3)$$

where $\mathrm{Re}_j = V_j d_j/\nu$ is the jet Reynolds number, and Sr_d is related to the swirl ratio as described above.

The present problem and experiment is then formulated according to Eq. (3), where Re_j is considered the independent variable, Sr_d the variable parameter, and D/d_j the constant parameter. The values of these parameters for the present experiment will be given in the next section.

Finally, it should be noted that the present formulation, Eq. (3), is only to first-order approximation in the range of immediate to high Reynolds number. Here, the effects of, e.g., surface tension, other geometric variables, and boundary layer characteristics, etc., are all neglected.

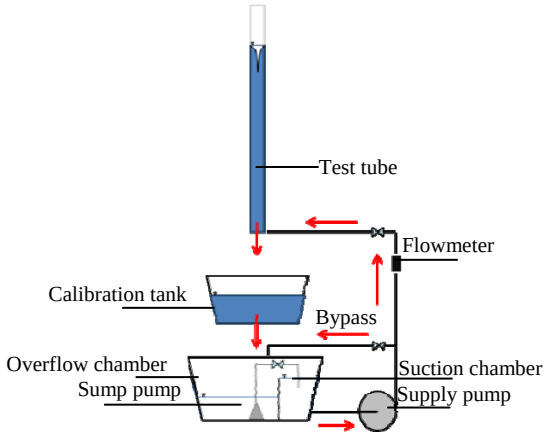

Fig. 2. Schematic diagram of the test rig.

3. Experimental Setup

In order to accommodate the wider range of α than [1], a new rig with longer vertical tube is constructed as shown schematically in Fig. 2. Water is pumped, with the supply pump, from the suction chamber of the suction tank. The suction tank is equipped with the overflow chamber in order to keep the suction head constant. On the discharge side of the supply pump is an ultrasonic flowmeter for flowrate measurement and an adjusting valve for flowrate adjustment. Due to the wide range of volume flowrate desired at the jet exit, from near zero to maximum, the bypass back to the overflow chamber is installed on the discharge side to help adjusting volume flowrate through the jet. After water is flowing through the jet and exiting the test tube through the bottom orifice plate, it is discharged to a calibration tank below. The lower side of the orifice plate is exposed to atmosphere. The calibration tank is used for calibrating the flowmeter as well as measuring volume flowrate by timing a volume of water. The water in the calibration tank is then drained to the overflow chamber of the suction tank, and the sump pump in the overflow chamber is used to pump water back to the suction chamber.

The vertical tube is acrylic with the inner diameter D of 74 mm and 2.6 m high. The jet has an inner diameter d_j of 6.2 mm, and there is a straight tube section of $25d_j$ long upstream of the jet exit to ensure a reasonable fully-developed flow at the jet exit. The jet exit is filed to match the curved inner surface of the tube. In order to adjust Sr_d, three interchangeable orifice plates with the orifice diameters of 6.2, 8.8, and 12.4 mm are used.

According to our problem formulation in Eq. (3), these result in the constant parameter D/d_j of 12 and the variable parameter Sr_d of 1, 2, and 4.

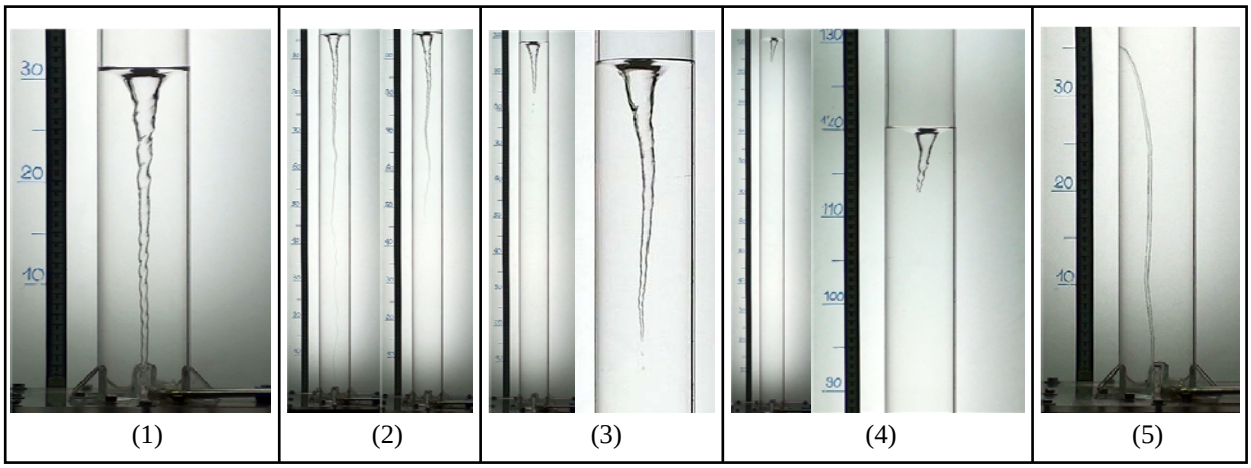

Fig. 3. Five flow regimes (1)-(5) [Regime 5: no vortex is not shown.], and (6) a 'reversed vortex', in case $Sr_d = 2$.

The volume flowrate is adjusted such that the independent variable, i.e., the jet Reynolds number Re_j, is varied from near zero to 100,000. From [1], anticipating the important role of $\alpha = \mathrm{Re}_j/Sr_d$ in place of Re_j and Sr_d separately, this translates into the range of α of near zero to 27,000, extending beyond 15,000 of [1]. The values of the parameters for each case of Sr_d are summarized in Table 1.

Table 1. Governing dimensionless parameters.

Sr_d	Re_j	α
1	4,200 – 24,000	4,200 – 24,000
2	9,000 – 54,000	4,500 – 27,000
4	17,500 – 98,000	4,375 – 24,500

An experiment is conducted via flow visualization with backlight. Video clips are taken with a commercial video camera. The vortex air core depth h and the water level H are measured with a scale, made from a commercial measuring tape installed on the backlight plate.

4. Results

4.1. Flow regimes

As the jet velocity is increased from zero, which corresponds to the increase in Re_j, the following five flow regimes are observed for each Sr_d, see Fig. 3. (Due to the limitation in the maximum volume flowrate of the system, for $Sr_d = 4$ we can observe upto flow Regime 3 only.)

Regime 1: Fig. 3(1): Vertically-steady, full-time fully-stretched vortex, $h/H = 1$.

When the jet velocity is low, which corresponds to low Re_j, the water level is steady - not oscillating - but low. The bathtub vortex is formed and is *always* fully stretched, with the vortex air core extending from the free surface at the top down through the orifice at the bottom, making the vortex stretching ratio h/H steady at one. In other words, the bathtub vortex is 'full-time fully stretched.'

Regime 2: Fig. 3(2): Vertically oscillating, partial-time fully-stretched vortex, $0 < h/H <= 1$.

When the jet velocity is further increased, which corresponds to the increase in Re_j, the water level further rises. However, the water level becomes unsteady, and vertically oscillating. The bathtub vortex is formed and accordingly becomes unsteady and vertically oscillating in a periodic manner. Specifically, the bathtub vortex is oscillating between the two states of fully stretched ($h/H = 1$) and partially stretched ($0 < h/H < 1$), the latter of which the vortex air core extends but does not reach the orifice at the bottom. In other words, the bathtub vortex is only 'part-time fully stretched.'

Additionally, the following observation can be made. When the vortex air core is extending down and reaching the orifice at the bottom, the water level starts rising. For a while then, the vortex air core starts retracting from the orifice, and the water level starts dropping. In other words, there is a correlation between the presence of the vortex air core at the orifice and the water level, or the periodic presence of the vortex air core at the orifice and the vertical oscillation of water level, though not exactly in phase. This can be explained in terms of the blockage effect of the vortex air core that blocks the effective water flow area at the orifice, the point that we will discuss further in Sec. 6: Blockage effects.

Regime 3: Fig. 3(3): Vertically steady, full-time partially-stretched vortex with air bubble detachment, $0 < h/H < 1$.

When the jet velocity is further increased, the water level further rises but now becomes steady – not oscillating. The bathtub vortex is formed and always only partially stretched ($0 < h/H < 1$); the vortex air core never reaches the orifice at the bottom. In other words, the bathtub vortex is 'full-time partially stretched.'

Additionally, discrete, relatively small air bubbles, are observed to periodically detach from the tip of the vortex air core and are convected down and out through the bottom orifice.

Regime 4: Fig. 3(4): Vertically steady, full-time partially-stretched vortex without air bubble detachment, $0 < h/H < 1$.

When the jet velocity is further increased, the water level further rises and is still steady. The flow in this regime is very much like Regime 3, i.e., the bathtub vortex is full-time partially stretched. Unlike flow Regime 3, however, there is no longer air bubble detachment.

Regime 5: Fig. 3(5) – not shown: No bathtub vortex, $h/H \approx 0$.

When the jet velocity is further increased, the water level further rises and is steady. There is no longer bathtub vortex formed, i.e., no discernible deformation of the free surface. From flow Regime 4 to 5, there is a gradual decrease in the vortex stretching ratio *h/H*. For practical purpose, though arbitrary, we may therefore consider the case in which h/H is less than some practical value to be in flow Regime 5. (For this reason, no marker is used to differentiate flow Regime 5 from Regime 4 in Fig. 4.)

Before we discuss the results further, some point should be noted. In some conditions of Sr_d and Re_j, the flow may exhibit the characteristics of both neighboring regimes, and the transition between regimes may not be abrupt. Hence, the identification of the flow regimes is not without difficulty. More discussions are given in Sec. 7: Discussions.

Flow Pattern 6: Fig. 3(6): Vertically oscillating, part-time 'reversed vortex'

A special flow pattern is observed in the case of Sr_d = 2 and Re_j around 60,000, corresponding to α around 30,000. Namely, at around this condition, instead of having an air core originating from the upper free surface extending down, we have an air core originating from the atmosphere under the orifice stretching up the height of the fluid column. The flow is periodic, or intermittent. The air core stretches up from below – but never reaches the free surface – and rotates about the tube center while the water level rises. Subsequently, the air core starts to retract and disappears completely while the water level drops again. The water level remains steady for a time, and then the phenomenon repeats, though not at an exact period. Like flow Regime 2, here we observe the correlation between the periodic presence of the air core at the orifice and the vertical oscillation of water level.

Finally, with the extended range of Re_j and Sr_d, hence α, the present results are consistent with [1]. Additionally, however, a new flow pattern, i.e., flow Pattern 6, is identified.

4.2. Vortex stretching ratio, *h/H*

Figure 4(a) shows the vortex stretching ratio (*h/H*), together with the normalized water level (*H/d*), as a function of Re_j at various Sr_d's according to Eq. (3). First note that while the uncertainties of these quantities depend on the flow regime, in order to give some indication we estimate the uncertainties in *h/H* to be ± 0.05; *H/d*, ± 10; and α, $\pm 2{,}000$.

For each Sr_d, the followings can be observed, see, e.g., at Sr_d = 4.

- The vortex stretching ratio relation *h/H*-Re_j can be divided into two regions. At low Re_j in flow Regime 1, *h/H* is constant at one. At higher Re_j beyond flow Regime 1, the relation can be approximated by a half-gaussian curve.
- As a result, there is a characteristic point on the curve as Re_j increases from zero, i.e., the point at the end of flow Regime 1 and the start of flow Regime 2, or the *cut-off point*, where the vertically steady, full-time fully-stretched vortex starts to retract and becomes vertically oscillating, part-time fully stretched vortex. Note that before this cut-off point (flow Regime 1), there is a full-time blockage effect of the vortex air core present at the orifice while after and beyond this point there is only part-time (flow Regime 2) or almost no or no blockage effect (flow Regimes 3 and beyond). This point is also the vertex of the half-gaussian curve.

Another interesting results can be observed when we compared *h/H*-Re_j relations at various Sr_d's.

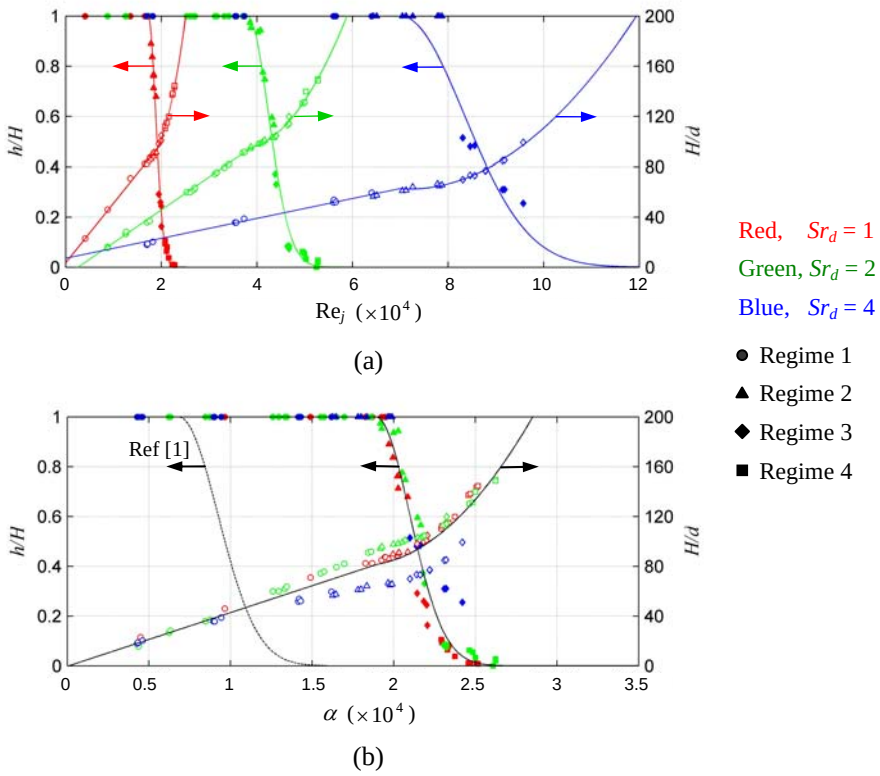

Fig. 4. Vortex stretching ratio (h/H) and normalized water level (H/d): (a) against Re_j at various Sr_d's, (b) against α. Dashed line in (b) is from [1]. Because of gradual decrease in h/H as the flow changes from Regime 4 to Regime 5, no marker is used to differentiate Regime 5 from Regime 4 in this figure.

- As Sr_d increases, the starting point for each flow Regime moves to a higher Re_j. For example, when Sr_d increases, the vertex of the half-gaussian curve (the cut-off point) moves to a higher Re_j.
- In addition, as Sr_d increases, the width of Re_j for any one flow regime also increases.
- Finally, as Sr_d increases, higher Re_j is required in order to cover all five flow regimes.

These observations on the dependence of Re_j on Sr_d for the occurrence of any one flow regime suggest to Rumpirujipong and Bunyajitradulya [1] that for the occurrence of any one flow regime there is a relation between Re_j and Sr_d, and they are not independent as formulated in Eq. (3). Examining the fact that as Sr_d increases, the starting point Re_j and the width of Re_j for each flow regime increases, they postulate a new variable α, defined as

$$\alpha = \frac{\mathrm{Re}_j}{Sr_d}, \qquad (4)$$

as the potential governing variable for the vortex stretching ratio h/H. They then plot h/H against α and found that all h/H-Re_j relations for various Sr_d's reasonably well collapse onto one h/H-α relation, independent of both Re_j and Sr_d separately.

Following the same scheme, we replot our results as h/H vs α as shown in Fig. 4(b). The present result shows that all h/H-Re_j relations for various Sr_d's reasonably well collapse onto one h/H-α relation, independent of both Re_j and Sr_d separately, consistent with [1]. However, the present result is inconsistent with [1] in that the h/H-α relation differs from [1], which is shown as the dashed line in the figure. Specifically, the present h/H-α curve is shifted to the right, to a higher α, when compared to [1]. This suggests that some other dimensionless parameters, which are not taken into account in the formulation Eq. (3) and are not equal in the two experiments, play a role. This point will be discussed further in Sec. 7: Discussions. At present, we give the two results for comparison.

Present result:

$$\frac{h}{H} = \begin{cases} 1, & \alpha < 18{,}900 \\ e^{-\left(\frac{\alpha - 18{,}900}{2{,}940}\right)^2}, & \alpha \geq 18{,}900 \end{cases} \qquad (5a)$$

From [1]:

$$\frac{h}{H}=\begin{cases}1, & \alpha<6{,}820\\ e^{-\left(\frac{\alpha-6{,}820}{3{,}400}\right)^2}, & \alpha\geq 6{,}820\end{cases} \quad (5b)$$

The cut-off points, or the vertex of the half-gaussian curve, for the present and past studies are at α = 18,900 and 6,820, respectively.

Finally, as Fig. 4(b) shows, by identifying each flow regime with the vortex stretching ratio *h/H*, the condition for the formation of bathtub vortex in each flow regimes is found to correlate fairly well with the parameter α, albeit with some inconsistency with [1].

4.3. Normalized water level, *H/d*

Figure 4(a) also shows the normalized water level (*H/d*) as functions of Re_j at various Sr_d's, according to Eq. (3). For each Sr_d, the followings can be observed, see, e.g., at Sr_d = 4.

The relation can be divided into two regions. Namely, in flow Regime 1, where there is full-time blockage effect of the vortex air core at the orifice, the normalized water level varies linearly and is increasing with the Reynolds number, $H/d \sim \mathrm{Re}_j$. This also indicates that in this flow regime, the water level is linearly proportional to the jet velocity, $H \sim V_j$.

Beyond flow Regime 1, i.e., approximately from Regimes 2 to 5, where there is only partial-time or no blockage effect from the vortex air core at the orifice, the normalized water level varies parabolically with the Reynolds number, $H/d \sim \mathrm{Re}_j^2$. This also indicates that in these flow regimes the water level is proportional to the square of the jet velocity, $H \sim V_j^2$. The relations in this regime are expectable, especially in flow Regimes 3 to 5 where there is virtually no blockage effect of the vortex air core at the orifice, and can be explained as follows. From the Bernoulli's equation, the draining velocity at the orifice is approximately proportional to the square root of the water level, or $H \sim V_e^2$. Because of the conservation of mass, the draining velocity is also linearly proportional to the jet velocity, $V_e \sim V_j$. As a result, we have $H \sim V_j^2$ and $H/d \sim \mathrm{Re}_j^2$.

With the collapse of h/H against α, we similarly plot H/d against α in Fig. 4(b) and find that H/d reasonably collapses against α, though not without some deviations; the tentative curve fit is shown and given by

$$\frac{H}{d}=\begin{cases}(4.314\times10^{-3})\alpha-0.3988, & \alpha<18{,}900\\ (1.069\times10^{-6})\alpha^2-(3.836\times10^{-2})\alpha+424.5, & \alpha\geq 18{,}900\end{cases} \quad (6)$$

Finally, when *H/d*-Re_j relations for various Sr_d's are compared (Figs. 4a and b), it is observed that the transition point from linear to parabolic relations for higher Sr_d (Sr_d = 4) occurs at lower *H/d* than at lower Sr_d. This point will be discussed in relation to the blockage effect of the vortex air core in Sec. 6: Blockage effects.

5. Flow Control Devices

As mentioned in the Introduction, our second objective in this study is to investigate a suitable flow control devices such that the formation of bathtub vortex can be prevented. As a result, a few configurations of the flow control devices are selected and tested. The criteria in choosing the devices are that they should 1) introduce minimal loss, and 2) be easy to make and install. This results in two devices: a cross made from thin flat plates (*D*/2 and *D*/4 high), Fig. 5(b)-(c), and a thin flat plate, or a strip, (*D*/4 high), Fig. 5(d), all span the diameter of the tube. The devices are tested at the condition considered to be the most severe, in flow Regime 1 where the vortex is full-time fully stretched. The tests are made for α from 6,200 to 18,400, the latter is near the end of flow regime 1 where water level is the highest in the regime. The devices are tested by installing them at two extreme positions, either near the tube floor or near the free surface. The test cases are shown in Table 2.

Table 2. Flow control devices test cases.

Sr_d	Re_j	α	Position above the tube floor
1	6,200	6,200	*D*/2
	9,100	9,100	
	13,500	13,500	*D*/2, 4*D*
2	17,600	8,800	1*D*
	27,000	13,500	
	36,900	18,400	1*D*, 6*D*

Flow Control Device Results

In all test cases shown in Table 2, all three devices can effectively get rid of the vortex and the vortex air core completely as shown as an example in Fig. 5 for case Sr_d = 1, α = 13,500, when the device is installed near the free surface.

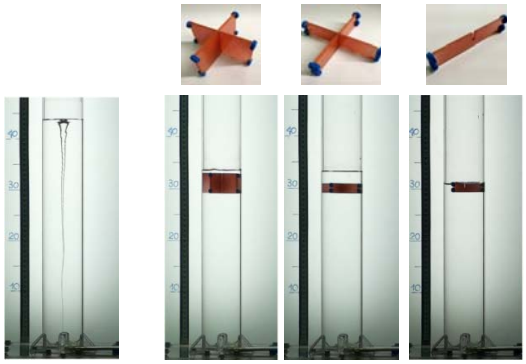

No FC device **With FC Device**

Device height:	*D*/2	*D*/4	*D*/4
(a)	(b)	(c)	(d)

Fig. 5. The effectiveness of the FC devices at Sr_d = 1 and α = 13,500: (a) no FC device, (b)-(d) with FC device installed near the free surface, at height $\approx 4D$.

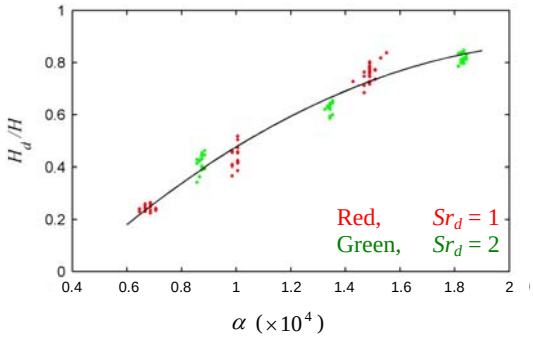

Fig. 6. Normalized water level reduction ratio, H_d/H, when flow control device is installed. The data included in this figure are all test cases shown in Table 2 and for both positions of the flow control devices, together with some repeated measurements.

Of particular note in Fig. 5 is the drop in water level when the device is installed and as a result the vortex air core through the orifice is gotten rid of, when compared to the case without the device. Note that all these cases are at the same α and volume flowrate. This is the case for all test cases. Figure 6 shows the normalized water level reduction ratio H_d/H against α, where H_d is the water level when the device is installed and H is the corresponding water level when no device is installed, for all test cases and with some repeated measurements. As can be seen, the result shows that as α increases, H_d/H increases towards one, though it may not, or may never, reach one.

Finally, like flow Regimes 2 and 6, it can be observed in flow Regime 1 with the flow control device installed here that the water level again correlates with the presence of the vortex air core through the orifice. When there is an air core through the orifice, the water level tends to rise high; and vice versa. This will be elaborated further in terms of the blockage effect in the next section.

6. Blockage effects of the vortex air core

The presence of the vortex air core at the orifice results in the reduction in the effective flow area of water, or the *blockage effect*. For clarity, we define the *effective flow area ratio* $r_A = (A - A_{block})/A$ and *the blockage area ratio* $r_b = A_{block}/A$, where A is the geometric area of the orifice and A_{block} is the cross sectional area of the vortex air core at the orifice.

On the oscillation of water level in flow Regime 2 and flow Pattern 6

It is observed that the oscillation in water level in flow Regime 2 and flow Pattern 6 correlates with the periodic presence of the vortex air core at the orifice. Specifically, when there is a vortex air core through the orifice, the water level tends to rise high; when there is none, the water level tends to drop low, though may not be exactly in phase. This can be explained in terms of the blockage effect of the vortex air core at the orifice as follows.

When there is an air core at the orifice, the air core blocks the effective flow area of water through the orifice. As a result, water starts to accumulate in the tube, causing the water level in the tube to rise high. The rising water level results in the increase in hydrostatic pressure, which in turn causes the smaller-diameter bottom portion of the air core near the orifice to collapse. Consequently, the vortex air core retracts from the orifice. The retraction of the vortex air core from the orifice then results in the increase in the effective flow area of water. Because of this increase, together with the high hydrostatic pressure head due to high water level, the draining rate of water from the tube then increases, causing the water level in the tube to drop low. As a result, the hydrostatic pressure decreases and this initiates the extension of the vortex air core down to the orifice again, and the cycle repeats.

On the lower normalized water level (*H/d*) at higher Sr_d

When H/d-Re_j relations for various Sr_d's are compared in Fig. 4, it is observed that the transition point from linear to parabolic relations,

i.e., roughly from flow Regime 1 to flow Regime 2, for higher Sr_d (Sr_d = 4) occurs at lower H/d than at lower Sr_d. The following explanation is offered.

Higher Sr_d has larger orifice diameter d than lower Sr_d while near the cut-off point (the boundary between flow Regimes 1 and 2) the diameter of the vortex air core at the orifice is small and relatively independent of Sr_d. As a result, the effective flow area ratio r_A of higher Sr_d is larger than lower Sr_d. Because of this larger effective flow area ratio, the water flow area of higher Sr_d at the orifice is closer to the actual geometric area of the orifice. Consequently, H/d of case of higher Sr_d exhibits the parabolic relation, the relation when there is no blockage, sooner, i.e., at lower H/d, than cases of lower Sr_d.

On the reduction of water level in flow Regime 1 when flow control device is installed

Similar explanation as above can be offered for the reduction in the water level in flow Regime 1 when the flow control device is installed and, as a result, the vortex air core gotten rid of as presented in Sec. 5.

Of particular note is the increase of the normalized water level reduction ratio H_d/H with α, shown in Fig. 6. This can be explained as follows. In flow Regime 1, as α increases, the diameter of the vortex air core at the orifice decreases; hence, the effective flow area ratio r_A increases. In other words, the effective flow area ratio r_A increases with increase in α. As a result, at higher α, when the flow control device is installed and the vortex air core gotten rid of, the reduction of the water level will be less (H_d/H closer to 1) than at lower α since its blockage due to the vortex air core is lower in the first place.

7. Discussions

During the course of our investigations, there are some interesting results and issues, which we now discuss.

Comparisons of flow regimes with past studies

It is insightful to compare various flow regimes identified in the present work and [1], [2, see also 3 and 5], and [6], albeit the fact that they are generated by different flow configurations and conditions as described in the Introduction. Most notable differences are

- intermittent [6] vs stationary [present work, 1,2],
- constant and controlled water level [2,6] vs variable and dependent water level [present work, 1],
- vertically distributed forcing tangential velocity [2,6] vs bottom, point forcing tangential velocity [present work, 1].

With these, some observations can be made.

- Excluding the case of no bathtub vortex, the flow regimes reported in both [2] and [6] are approximately equivalent to flow Regimes 4, 3, and 1.
- Intermittency aside, as far as the vortex air core and bubble detachment are concerned, characteristically the dimple in [6] is equivalent to flow Regime 4; Type I to Regime 3; and Type II to Regime 1.
- Due to the controlled water level in both [2] and [6] as opposed to the uncontrolled in the present work and [1], [2] and [6] naturally did not observe flow Regime 2: the *vertically oscillating*, part-time fully-stretched vortex, as observed here and in [1].

The similarity of flow regimes in the present work and past works also has an implication in terms of the condition for the formation of a bathtub vortex that we discuss next.

The condition for the formation of a bathtub vortex and the effective flow control scheme

Following [1] and according to the premise as stated in the Introduction, the present result shows that under appropriate condition (say, appropriate range of α) a bathtub vortex can form even in the case of a point forcing near the bottom. Nonetheless, for each flow Regimes 1 to 4, the point forcing has a limitation upto a certain normalized water level H/d at which each flow regime eventually ends (Fig. 4b).

Furthermore, for this configuration of a cylindrical container with centered orifice, the present together with the past results indicate that, neither a uniform forcing along the depth of the body of fluid nor the point forcing near the bottom is – by themselves - necessary for the formation of a bathtub vortex, from flow Regime 1 to flow Regime 4. Instead, these results (as well as observations of naturally occurring phenomena such as draining a tank) suggest that the condition for the formation of a bathtub vortex is localized and depends more on the condition of the flow in a localized vertical cylindrical region along the depth of the body of fluid, centered along the container axis. This conjecture is partly supported

by the fact that the flow control devices in Sec. 5 are effective both when installed at the topmost position near the free surface and at the bottommost position near the orifice.

The difficulty in identifying flow regimes with fully-stretched state

As the Reynolds number is increased towards the end of flow Regime 3, the identification of the flow Regime 3 with air bubble detachment is fairly obvious. Namely, the vortex air core is relatively short such that the tip of the vortex air core is clearly high above the bottom orifice, and discrete, relatively small, air bubbles are clearly seen to periodically detach from the tip of the vortex air core and travel a depth of water down and out the orifice at the bottom.

In other cases of Reynolds number, however, the distinction between flow Regimes 2 and 3, and even 1, is not without difficulty. More specifically and especially, as Re_j is increased towards the end of the flow regime with full-time or partial-time fully-stretched state, i.e., Regimes 1 and 2, the lower part of the vortex air core in the fully-stretched state may be so thin in diameter such that it is unsteadily being sheared or collapsed apart into pieces along its length. As a result, this at times appears as thin longitudinal air bubbles, or air tubes, being convected down and out the bottom orifice, a little like flow Regime 3.

In this regard, for the demarcation and identification of flow regimes, we identify the characteristic of the flow regime 1 as being full-time, fully-stretched (h/H is full-time one), while the characteristic of the flow regime 3 as with the tip of the vortex air core being clearly high above the bottom orifice and with discrete, relatively small, air bubbles detaching from the tip of the vortex air core and travelling a depth of water down and out the orifice at the bottom.

The discrepancy in *h/H*-α relations between the present result and [1]

As described in Sec. 4.2, while the present result is consistent with [1] in the collapse of *h/H*-Re_j relations for various Sr_d's onto one *h/H*-α relation, it is inconsistent with [1] in the exact *h/H*-α relation itself. Namely, the present curve is shifted to the right, i.e., towards higher α, when compared to [1] as shown in Fig. 4(b).

To preliminary investigate this, we go back and re-examine the past and present experiments and the test rigs and find some differences in the two setups, namely 1) the vertical gap of the jet from the floor (Δ_z), and 2) the radial gap of the jet from the tube wall (Δ_r). Specifically, the normalized vertical gap Δ_z/d_j of the present experiment (≈ 1) is larger than [1] (≈ 0), and the normalized radial gap Δ_r/d_j of the present experiment (≈ 0) is smaller than [1] (≈ 2).

With this, we postulate that the difference in the gaps can cause the difference in the effective velocity of the jet due to the wall and boundary layer effects. In this regard, in order to preliminarily examine the effect of the vertical gap Δ_z in this setup, which can be done much simpler by using filler plates to narrow the vertical gap at the bottom of the jet, we do additional experiments in cases Sr_d = 1 and 2 by partially filling the vertical gap with filler plates. As a result of the filling, the modified setup is more similar to [1]. Our preliminary data show that a few new *h/H*-α data points with the filler plates do move to the left of the original curve in Fig. 4(b), making the present *h/H*-α curve more consistent with [1]. Nonetheless, more detailed examinations are required before the discrepancy can be satisfactorily explained.

8. Conclusions

The condition under which a bathtub vortex is formed and the characteristics of the formed bathtub vortex generated by tangential jet injection at the bottom of a vertical tube with draining orifice are investigated. Five flow regimes and one additional flow pattern are identified (Sec. 4.1). By identifying each flow regime with the vortex stretching ratio *h/H*, the condition for the formation of bathtub vortex in each flow regimes is found to correlate reasonably well with the parameter α (Sec. 4.2). The collapses of the vortex stretching ratio *h/H* and the normalized water level *H/d* against α, independent of the jet Reynolds number Re_j and the diametric swirl ratio Sr_d separately, are confirmed, but with some discrepancy from [1] (Secs. 4.2 and 4.3). The parameters that may cause the discrepancy are discussed (Sec. 7). A flow control device for the prevention of bathtub vortex formation in the shape of a small strip installed at either the topmost position near the free surface or the bottommost position near the orifice is both found to be effective (Sec. 5). This suggests that the condition for bathtub vortex formation is localized in the vertical cylindrical region centered on the container axis and that an effective flow control scheme for its prevention can focus on a localized disturbance in this localized region (Sec. 7). Finally, many bathtub

vortex related phenomena such as the oscillation of water level in flow Regimes 2 and flow Pattern 6, and the reduction in water level when flow control device is installed and the vortex air core gotten rid of, are identified and explained in terms of the blockage area ratio when the vortex air core is present at the orifice (Sec. 6).

9. References

[1] Rumpirujipong, K. and Bunyajitradulya, A. (2011). Condition and characteristic for bathtub vortex generated by tangential injection in a vertical pipe, TSF-44, paper presented in *The Twenty-Fifth Conference of Mechanical Engineering Network of Thailand*, October 19-21, 2011, Krabi, Thailand. (In Thai.)

[2] Andersen, A., Bohr, T., Stenum, B., Juul Rasmussen, J., and Lautrup, B. (2003). Anatomy of a bathtub vortex, *Physical Review Letters*, Vol. 91, No.10, 104502.

[3] Andersen, A., Bohr, T., Stenum, B., Juul Rasmussen, J., and Lautrup, B. (2006). The bathtub vortex in a rotating container, *Journal of Fluid Mechanics*, Vol. 556, pp. 121-146.

[4] Lundgren, T. S. (1985). The vortical flow above the drain-hole in a rotating vessel, *Journal of Fluid Mechanics*, Vol. 155, pp. 381–412.

[5] Bergmann, R., Andersen, A., Van der Meer, D., and Bohr, T. (2009). Bubble pinch-off in a rotating flow, *Physical Review Letters*, Vol. 102, 204501.

[6] Ezure, T., Kimura, N., Miyakoshi, H., and Kamide, H. (2011). Experimental investigation on bubble characteristics entrained by surface vortex, *Nuclear Engineering and Design*, Vol. 241, pp. 4575-4584.

[7] Monji, H., Shinozaki, T., Kamide, H., Sakai, T. (2010). Effect of experimental conditions on gas core length and downward velocity of free surface vortex in cylindrical vessel, *Journal of Engineering for Gas Turbines and Power*, Vol. 132, 012901.